Geoscience Frontiers xxx (xxxx) xxx

HOSTED BY

Contents lists available at ScienceDirect

Geoscience Frontiers

journal homepage: www.elsevier.com/locate/gsf

Research Paper

Use of geospatial tools to predict the risk of contamination by SARS-CoV-2 in urban cemeteries

Paloma Carollo Toscan [a], Alcindo Neckel [a,*], Laércio Stolfo Maculan [a], Cleiton Korcelski [a], Marcos L.S. Oliveira [b,c], Eliane Thaines Bodah [d,e], Brian William Bodah [e], Henrique Aniceto Kujawa [f], Affonso Celso Gonçalves [g]

[a] Faculdade Meridional, IMED, 304, Passo Fundo, RS 99070-220, Brazil
[b] Department of Civil and Environmental, Universidad de la Costa, CUC, Calle 58 # 55–66, Barranquilla, Atlántico, Colombia
[c] Universidad de Lima, Departamento de Ingeniería civil y Arquitectura, Avenida Javier Prado Este 4600, Santiago de Surco 1503, Peru
[d] State University of New York, Onondaga Community College, 4585 West Seneca, Turnpike, Syracuse, NY 13215, USA
[e] Thaines and Bodah Center for Education and Development, 840 South Meadowlark Lane, Othello, WA 99344, USA
[f] University of Perugia, Piazza Università, 1, 06123 Perugia, Italy
[g] State University of Western Paraná – UNIOESTE, Center of Agrarian Sciences, Rua Pernambuco, 1777, Centro, Marechal Cândido Rondon, PR 85960-000, Brazil

ARTICLE INFO

Article history:
Received 28 April 2021
Revised 15 August 2021
Accepted 26 September 2021
Available online xxxx

Keywords:
Remote sensing
Reflectance temperature
Atmospheric contamination
Urban environment
SARS-CoV-2

ABSTRACT

Urban cemeteries are increasingly surrounded by areas of high residential density as urbanization continues world-wide. With increasing rates of mortality caused by the novel coronavirus, SARS-CoV-2, urban vertical cemeteries are experiencing interments at an unprecedented rate. Corpses interred in the 3rd to 5th layer of vertical urban cemeteries have the potential to contaminate large adjacent regions. The general objective of this manuscript is to analyze the reflectance of altimetry, normalized difference vegetation index (NDVI) and land surface temperature (LST) in the urban cemeteries and neighbouring areas of the City of Passo Fundo, Rio Grande do Sul, Brazil. It is assumed that the population residing in the vicinity of these cemeteries may be exposed to SARS-CoV-2 contamination through the displacement of microparticles carried by the wind as a corpse is placed in the burial niche or during the first several days of subsequent fluid and gas release through the process of decomposition. The reflectance analyses were performed utilizing Landsat 8 satellite images applied to altimetry, NDVI and LST, for hypothetical examination of possible displacement, transport and subsequent deposition of the SARS-CoV-2 virus. The results showed that two cemeteries within the city, cemeteries A and B could potentially transport SARS-CoV-2 of nanometric structure to neighboring residential areas through wind action. These two cemeteries are located at high relative altitudes in more densely populated regions of the city. The NDVI, which has been shown to control the proliferation of contaminants, proved to be insufficient in these areas, contributing to high LST values. Based on the results of this study, the formation and implementation of public policies that monitor urban cemeteries is suggested in areas that utilize vertical urban cemeteries in order to reduce the further spread of the SARS-CoV-2 virus.

1. Introduction

Urban cemeteries, according to Abia et al. (2019) and Neckel et al. (2021) have been recognized as potential pollutant reservoirs, responsible for directly contaminating the environment as the corpses interred within decompose. This pollution has the potential to negatively compromise the health of the population residing in neighborhood areas directly adjacent to the cemetery. The natural process of decay attracts insects which create larval masses once their eggs hatch on the decaying material (Mikszewski et al., 2021). The process also produces odors and releases volatile gases into the immediate atmosphere, some of which harm human health (Zorzi et al., 2021). Nanoparticles are extremely susceptible to transport by the wind, having been shown to remain airborne and travel for thousands of kilometers under certain circumstances (Blanar and Prada-Tiedemann, 2020).

The gases emitted by cadavers originate from microorganisms that decompose organic matter, producing 400 types of chemical and gaseous compounds, some of which are extremely toxic to

* Corresponding author.
E-mail address: alcindo.neckel@imed.edu.br (A. Neckel).

https://doi.org/10.1016/j.gsf.2021.101310
1674-9871/

humans (Balta et al., 2020; Blanar and Prada-Tiedemann, 2020). Neckel et al. (2021) demonstrated that the lack of treatment of these gaseous elements leads to the accumulation of contaminants in the localized atmosphere as the natural process of decay proceeds. Silva et al. (2020), Duarte et al. (2021) and Oliveira et al. (2021) warn that gases and other contaminants are added to Accumulated Ultrafine Particles (UFPs) and Nanoparticles (NPs) that are easily transported to other regions through wind action, spreading these harmful contaminants far and wide.

It is worth remembering that cities with high levels of air pollution have low air quality, increasing the likelihood of COVID-19 for humans exposed to the SARS-CoV-2 virus, and may also increase the severity of the disease (Barcelo, 2020; Shao et al., 2021). Thus, air pollution becomes a facilitator for the proliferation of SARS-CoV-2, when viral particles are present in nanoparticles, together in the gas structures dispersed in the air (Barcelo, 2020; Lalwani and Gautam, 2021; Stern et al., 2021). The SARS-CoV-2 virus, UFPs and NPs are all easily transported by wind as each has a diameter less than 2.5 μm. This allows them to remain suspended in the atmosphere for long periods of time (Barcelo, 2020; Cao et al., 2021; Oliveira et al., 2021; Shao et al., 2021).

The World Health Organization (WHO) reported on October 16, 2020 that the SARS-CoV-2 world-wide COVID-19 pandemic had reached 235 countries and had resulted in 1.09 million deaths (Anand et al., 2021). By March 31, 2021, the global death toll had exceeded 2.8 million. Nearly 318,000 of these deaths took place SARS-CoV-2 in Brazil as of March 31st (WHO, 2021).

The COVID-19 has been shown to attack nearly every system in the human body; however, the most deadly symptom to date consists of acute respiratory distress syndrome SARS-CoV-2 (Cao et al., 2021; Jansi et al., 2021; Moreno and Gibbons, 2021). As the SARS-CoV-2 virus has traversed the globe in record time and infected so many people, certain areas of the world are seeing infection and death rates that overwhelm not only hospital services but also burial grounds.

According to Neckel et al. (2021), the vast majority of urban cemeteries in Brazil consist of concrete mausoleum structures up to five stories tall with row upon row of interment niches, one atop another, referred to as vertical cemeteries. The practice of embalming is not widespread in Brazil, and the vast majority of bodies decay naturally through skeletonization of the remains. The close proximity of so many decaying corpses in these urban cemeteries generate high levels of gas release (Neckel et al., 2021; Stern et al., 2021).

The applicability of this study in the cemeteries of the City of Passo Fundo, and its surrounding areas, is justified by considering the greatly increased burial burdens presented by the COVID-19 pandemic. Calmon (2020) examined the increase of deaths in the largest city in Latin America, São Paulo, Brazil, which exhibited a 30% increase in burials in 2020, and in just one urban cemetery studied, an average of 100 burials were conducted daily. The steady deposition of contaminated corpses, combined with the microscopic size of the SARS-CoV-2 virus, the gaseous emissions that occur in early stages of decomposition, and the elevation of the burial structures hypothetically make it possible for airborne particles containing active SARS-CoV-2 to leave the vicinity of these urban cemeteries and enter adjacent residential areas. Toscan et al. (2020) showed that the examination of an area's altimetry, normalized difference vegetation index (NDVI) and land surface temperature (LST) made it possible to predict the likelihood of particle transport. We utilize these methods to predict the potential transport of SARS-CoV-2 from urban cemeteries to surrounding regions.

SARS-CoV-2 Altimetry is applied in the area of geosciences, when considering remote sensing in relation to the ability to assess different terrestrial representations at local and global scales, thus highlighting characteristics aimed at technical assessments, using radar altimetric data, obtained through electromagnetic reflectance waves captured by satellites (Rosmorduc et al., 2020; Toscan et al., 2020). For Cazenave (2019) and Gasparin et al. (2021), altimetry consists of high-precision geospatial technology, made available by Remote Sensing techniques, in order to assist in the topographic observation of the Earth's surface, considering the sea level as zero altitude (0), positive values of altitudes above sea level and negative below sea level, phenomena that become responsible for influencing the displacement and speed of the winds, dividing the variation in altimetry.

The NDVI is a measure of living vegetation, whose value is determined by the reflection of terrestrial chlorophyll (Gozdowski et al., 2020; Moreno et al., 2020). According to Ahmed and Singh (2020), Costa et al. (2020) and Moreno et al. (2020), NDVI is captured by satellites, through the spectral features of vegetation that emit wavelengths, represented by photosynthetic pigments, derived from the internal structure and the amount of water present in the vegetation. According to Li et al. (2021) the countless conditions of the Earth's surface climate dynamics are captured by electromagnetic waves, which can vary due to the presence of shadow, lighting geometry and meteorological conditions in the atmosphere. This is able to influence the temperature of terrestrial emissivity.

In this relationship, satellite images derived from the reflectance captured by electromagnetic wavelengths become extremely important to estimate the LST, resulting from data gathered on the reflectance temperature of the Earth's surface and the air temperature, which enable spectral mapping the spatial distribution of LST (Chatterjee et al., 2017; Sussman et al., 2019; Alexander, 2020; Guha et al., 2020; Cilek and Cilek, 2021; Li et al., 2021). These emissivity temperature variations vary by the intensity of the wind direction, inclination of incoming solar radiation and certain characteristics of the surface elements that propagate in different electromagnetic wavelengths (Nega et al., 2019; Alexander, 2020; Das and Das, 2020).

According to Alexander (2021) and Yang et al. (2021), the use of LST is able to estimate terrestrial temperature in small, medium and macro-regions. The LST displays color-code the temperature of the Earth's surface. Higher temperatures are represented on maps in reddish tones, while lower temperatures are represented by bluish tones (Zullo et al., 2019; Yang et al., 2021). Toscan et al. (2020) highlight the importance of conducting studies in urban cemeteries involving LST together with NDVI and altimetry, as they interact together in the environment to impact circulation of the wind.

Barcelo (2020) and Cao et al. (2021) have shown that the movement of airborne SARS-CoV-2 ultrafine particles of gaseous elements can be hindered, slowed, or even stopped through the presence of vegetation. Acting as a windbreak, the physical structure of vegetation serves as a natural barrier, slowing wind and providing surface area for potential particle deposition. In the case that these particles contain the SARS-CoV-2 virus, areas of high NDVI may significantly slow viral proliferation through wind action downwind of a contaminated source. Furthermore, Toscan et al. (2020) point out that the presence of NDVI is a catalyst for the temperature of terrestrial emissivity. Elevated LSTs accelerate the rate of decomposition of corpses in cemeteries. The timeframe of gaseous release is particularly relevant when dealing with a virus that has a limited lifespan outside of its host or within a deceased host.

The general objective of this manuscript is to analyze the reflectance of altimetry, normalized difference vegetation index (NDVI) and land surface temperature (LST) in the urban cemeteries and neighbouring areas of the City of Passo Fundo, Rio Grande do Sul, Brazil. The study appropriated previously unpublished satellite

images made available directly by NASA and USGS, which demonstrates the high degree of reliability and novelty of the geospatial applications carried out in this manuscript. The altimetry is analyzed in relation to the terrestrial dynamics of emissivity, in order to determine the possibility of exposure of the resident population living near these cemeteries to SARS-CoV-2 viral particles through the displacement of ultrafine particles, shed by the recently deceased and interred, and easily transported by the wind.

2. Materials and methods

2.1. Study area

The City of Passo Fundo is located in the Northwest region of the State of Rio Grande do Sul (far southern region of Brazil). It comprises an area of just under 781 km^2 and has an estimated 2021 population of just over 203,000 residents. The resulting demographic density of the city is roughly 385 residents / km^2 (IBGE, 2021). The City of Passo Fundo has an average annual growth rate of 1500 new inhabitants. This is due to the presence of industry, agribusiness, education and healthcare which together provide manpower and direct and indirect services that favor the development of the local economy (IBGE, 2021).

The climate of Passo Fundo is classified as being located in the fundamental temperate (C) and humid fundamental (f) climactic zone, with an average summer temperature above 22 °C (the average annual wind speed is 4.1 m/s (NE)), ranging from 660 to 700 m in height (Bonatti et al., 2019; Wanderley et al., 2019; Embrapa, 2021; Maroni et al., 2021). The native ecosystem in this area consists of the vegetation of the Atlantic Forest, with arboreal specimen of mixed rainforest, which currently only exists in fragmented areas outside of the urban perimeter (Neckel et al., 2020; Maroni et al., 2021). Much of Passo Fundo is surrounded by areas of agricultural production.

Passo Fundo contains five urban cemeteries within the city limits: Vera Cruz (A), Petrópolis (B), Ribeiros (C), Jardim da Colina (D) and Roselândia (E) (Fig. 1). Cemeteries C, D and E are located mainly on the outskirts of the modern city. Cemetery A was founded in January 1902, whereas cemetery B first opened in the mid 1960s. At the time of their construction, neither cemeteries A nor B were surrounded by residential areas. As the city has grown and expanded, both now find themselves surrounded by very dense residential areas. As the city continues to grow, this will also happen to cemeteries C, D and E.

The urban cemeteries of Passo Fundo, like all others on a global scale, play an indispensable role in meeting the burial demands of the local population. Throughout Brazil today, there are fewer and fewer spaces available for interment in urban cemeteries (Neckel et al., 2021). In 2019 Passo Fundo recorded a total of 3988 deaths. Current projections by the city's Health Department predict SARS-CoV-2 this number will increase by 20.4% in 2021, largely due to COVID-19 (PMPF, 2021).

2.2. Analytical methods

Analysis of the altimetry conditions, NDVI and LST applied to the urban cemeteries of Passo Fundo were delimited in radii extending 100, 300 and 500 m from the geographic center of each cemetery (point 0), following the distance parameters laid out by Neckel et al. (2017), Toscan et al. (2020) and Neckel et al. (2021), which determined a maximum potential radius of contaminant release by urban cemeteries at 500 m. This distance does not apply to UFPs, NPs or gaseous compounds/elements, which can travel great distances through wind action (Oliveira et al., 2021). These ultrafine particles are also capable of carrying the SARS-CoV-2 virus (Anand et al., 2021; Cao et al., 2021; Shao et al., 2021). For a better visualization of the analyzed perimeter, the Google Satellite background images were used during the preparation of the maps in the QGIS software. The spectral reflectance on the maps were generated from unpublished satellite images made available by NASA and USGS.

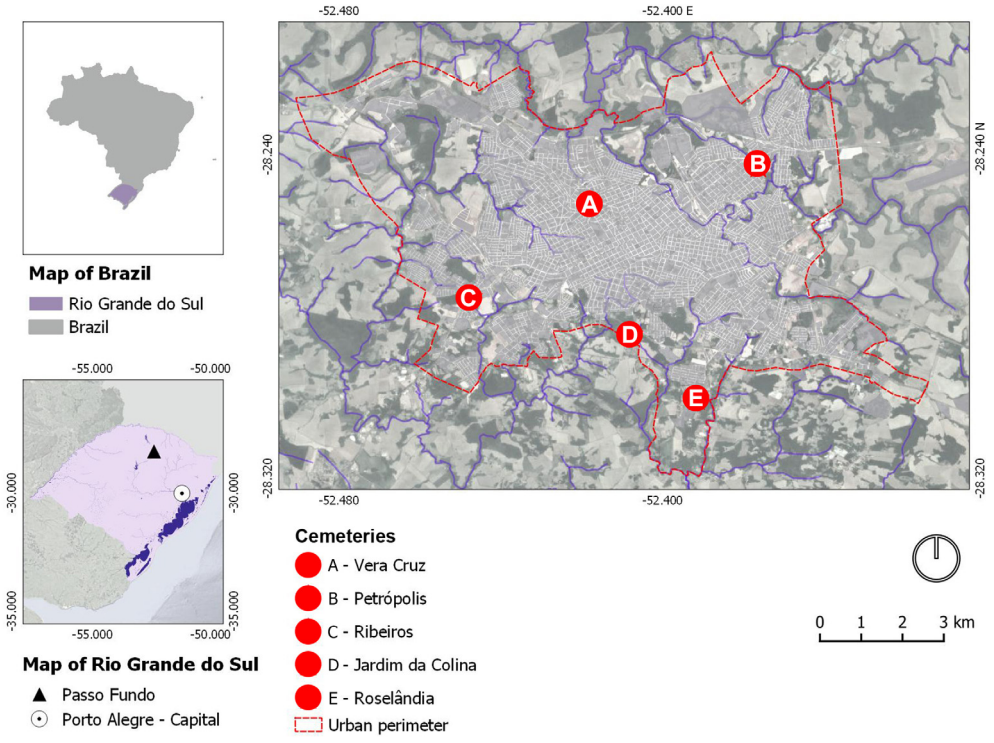

Fig. 1. Map of Passo Fundo, RS (southern Brazil) and its five urban cemeteries. Source: Based on data from IBGE (2021).

In this study, the physical dynamics of the environment related to altimetry, NDVI and LST were structured in a sequential manner dependent on the dates that Landsat 8 satellite images of the area were available, together with image treatment, data collection and statistical treatment of spectral data (USGS, 2021). The procedures for LST analysis were performed using data from the Landsat 8 satellite, with band 10 of the TIRS sensor. To understand the climactic dynamics of temperature in the urban cemeteries of Passo Fundo in relation to their surrounding areas, tools from QGIS 2.18 software were used to insert satellite images provided by the U.S. Geological Survey (USGS) in coordination with the National Aeronautics and Space Administration (NASA), which operates and distributes data from Landsat 8 satellites on a global scale (USGS, 2021). According to Rodriguez-Galiano et al. (2012) and Chemura et al. (2017), the Landsat 8 satellite images provide remote sensing data in order to facilitate the monitoring of the total reflectance of the Earth's surface. Since the choice of types of Landsat 8 satellite images worked on in this study prioritized the absence of cloud cover and the location of the images on path 220 and on line 80, images obtained on April 8, 2013 and March 17, 2020 were utilized. The images went through the redesign process using Datum bands of origin WGS 84 UTM 22N for the Datum Sirgas 2000 UTM 22S.

The analysis of the soil altimetry used images from Landsat 8 superimposed on the raster background of the Shuttle Radar Topography Mission (SRTM) program, with a 30 m spatial resolution, obtained from the USGS and projected along the base of the ground. Earth Explorer is where altimetry dimensions on the terrestrial plane were represented. The image utilized is identified as SRTM1S29W053V3, with a date of acquisition of February 11, 2020. The collection of attributes and values of the raster layers were performed using the Plugin Point Sampling Tool. For this, a layer of points was created, located at specific distances (Nascimento et al., 2021). The geographic central point of each cemetery was identified and radii of 100, 300 and 500 m were measured. The plugin created a new layer of points with locations given by the sampling points and attributes taken from the raster cells.

The climactic mappings referring to the LST were elaborated based on the information derived from the Landsat 8 data, for the calculation of the spectral radiance of the opening sensor in watts (Eq. (1) in Table 1), used the images of Bands 4 and 5 for Near Infrared Sensors (NIR) and band 10 for the use of the Thermal Infrared Sensor (TIRS). Afterward, the Gray Level (NC) image was converted to reflectance radiance (Table 1) (Rodriguez-Galiano et al., 2012; Vanhellemont, 2020). For the conversion of radiance to reflectance (Brightness temperature - BT) (Eq. (2) in Table 1), the digital numbers (DN) were converted to reflection using the data from the TIRS band in the form of spectral radiance for the reflectance temperature. Two constant variables were used, with the following metadata: the value K1 and K2, with the use of an algorithm to convert the reflectance to reflectance temperature (Rodriguez-Galiano et al., 2012; Toscan et al., 2020).

The NDVI method for correction of emissivity reflected by the vegetation existing both in the cemeteries of Passo Fundo and their surrounding areas, used the calculation of Eq. (3) (Table 1), which refers to the importance of the factor to infer the general condition of the vegetation, with the use of Bands 4 and 5 based on the NIR (Rodriguez-Galiano et al., 2012; Chemura et al., 2017). Then, based on Rodriguez-Galiano et al. (2012) and Chemura et al. (2017), the calculation of the proportion of vegetation was used: Pv is calculated according to Eq. (4) (Table 1).

The earth surface emissivity calculation (Eq. (5)) represented by Table 1 was applied, as it is necessary to understand the Earth surface emissivity (ε) to know how to estimate the LST, since the

Table 1
Equations made from the use of Landsat 8 images, using Bands 4 and 5 for Near Infrared Sensors (NIR) and band 10 for the use of the Thermal Infrared Sensor (TIRS).

Eq.	Formula	Equation variables
(1)	Lʎ = ML * Qcal + AL	Lʎ – Spectral radiance of the sensor ML – Scaling factor (0.0003342) Qcal – Band 10 image AL – Adaptive value specific to the scale of the rescaling factor (0.1)
(2)	BT = {k2 / [ln *(K1/ Lʎ) + 1]} – 273.15	BT – Brightness Temperature K1 – Band-specific constant conversion value (774.89) k2 – Band-specific constant conversion value (1321.08) Lʎ – Result of the first raster calculation (raster = TOA) ln – Raster calculator operation 273.15 – Value to convert temperature in Kelvin to °C
(3)	NDVI = (NIR – RED) / (NIR + RED)	NDVI – Normalized Difference Vegetation Index NIR – Near infrared RED – Bands of red
(4)	Pv = Square (NDVI - NDVI MIN) / (NDVI MAX - NDVI MIN)	Pv – Proportion of vegetation NDVI – NDVI raster NDVI MIN – Minimum NDVI value NDVI MAX – Maximum NDVI value
(5)	Eʎ = Evʎ* Pv + Esʎ (1- Pv) + C ʎ	Eʎ – Calculated emissivity Evʎ – Emissivity of vegetation Esʎ – Emissivitiy of soil C ʎ – Surface roughness Pv – Proportion of vegetation
(6)	p = h (c/ σ)	σ – Boltzmann constant (1.38×10^{-23} J/K) h – Plank's constant (6.626×10^{-34}) c – The speed of light (2.998×10^{8} m/s)
(7)	LST = BT / {1 + [(ʎ*BT/ ρ)*lnEʎ]}	LST – Land Surface Temperature Ts – Emissivity correlation (in °C) BT – At-sensor raster (in °C) ʎ – Wavelength of the emitted radiance (10.985) Eʎ - Calculated emissivity (ítem 6) ln – Operation raster calculator ρ – 1.4388

Earth surface emissivity is a proportionality factor of the blackbody's brightness (Planck's law) to predict the emitted brightness, and is the efficiency of transmitting thermal energy over the surface in the atmosphere (Rodriguez-Galiano et al., 2012; Chemura et al., 2017; Zullo et al., 2019; Toscan et al., 2020). The variance analysis of reflectance demonstrates the difference in surface temperature, altimetry and NDVI. The study warns of possible SARS-CoV-2 virus contamination based on the literature, being related to urban cemeteries as a possible source of viral proliferation.

Through statistical analysis (mean analysis) it was possible to tabulate these quantitative data, whose values were represented in an Excel spreadsheet (database), with the help of JASP software, version 0.13.01, through the analysis of descriptive statistics (King and Eckersley, 2019; Herbst et al., 2020). In this sequence, Pearson's correlation analysis was generated, capable of generating values for "r" between 1 and −1, with values close to zero meaning null correlation, with no influence between variables. The closer the value was to 1 meant that the increase of one variable causes the increase of the other. Meanwhile, values close to −1 means that increasing one variable decreases the other. As for interpretation, the correlation from 0.00 to 0.19 is considered very weak, 0.20 to 0.39 is weak, 0.40 to 0.69 is moderate, 0.70 to 0.89 is strong and 0.90 to 1 is very strong (Bermudez-Edo et al., 2018; Edelmann et al., 2021). Statistically the study showed high significance among the analyzed variables.

3. Results and discussion

3.1. Altimetry applied to urban cemeteries and the surrounding area

The altimetry analysis using Landsat 8 satellite data from 2020 show that the Vera Cruz (A) and Petrópolis (B) cemeteries are situated among the highest elevations found in the City of Passo Fundo. Cemeteries Ribeiros (C), Jardim da Colina (D) and Roselândia (E) meanwhile, are located at lower topographic levels (Fig. 2). Costa et al. (2010) and Toscan et al. (2020) have shown that altimetry is an important factor in the analysis and understanding of dynamics of relief in relation to its influence on the exposure of winds that move with greater intensity in terrestrial environments at higher attitudes. These stronger winds have a tendency to disperse contaminants susceptible to wind action found within a given area.

Silva et al. (2020) and Oliveira et al. (2021) highlight that windborne atmospheric contaminants tend to accumulate in UFPs and NPs (Fig. 3A). This displacement of atmospheric UFPs and NPs ((Cao et al., 2021) Anand et al., 2021; Shao et al., 2021), may provide a vector on which the SARS-CoV-2 virus can travel to surrounding communities. Zhu et al. (2020), has shown that the size

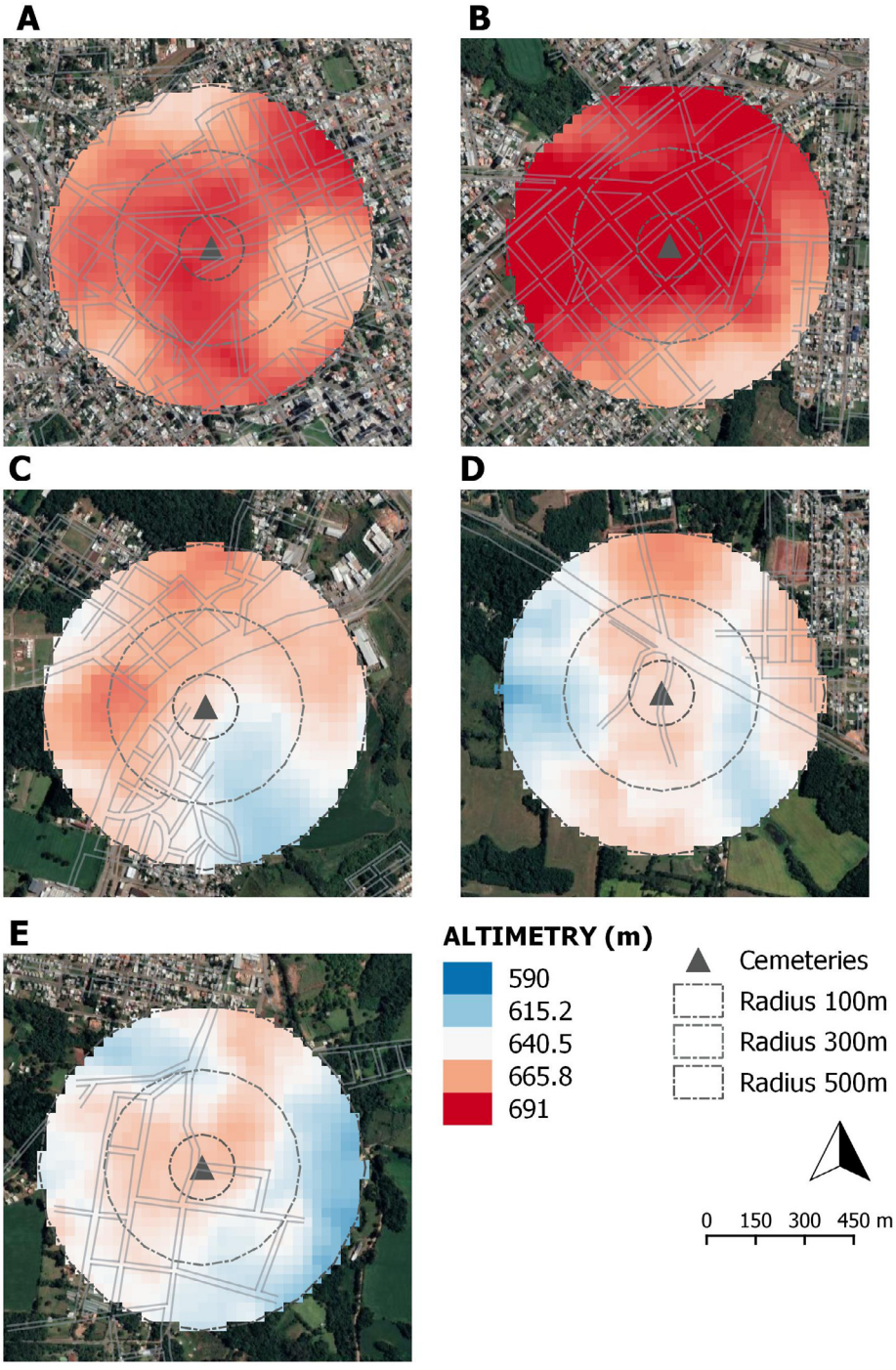

Fig. 2. Altimetry maps, using the Landsat 8 satellite from 2020, projected on Google Earth images, applied to urban cemeteries and their surroundings (radii of 100, 300 and 500 m) in Passo Fundo / RS. Cemeteries: Vera Cruz (A), Petrópolis (B), Ribeiros (C), Jardim da Colina (D) and Roselândia (E). Source: Adapted from the IBGE database (2021), USGS (2021), with overlay on Google Earth images (2021).

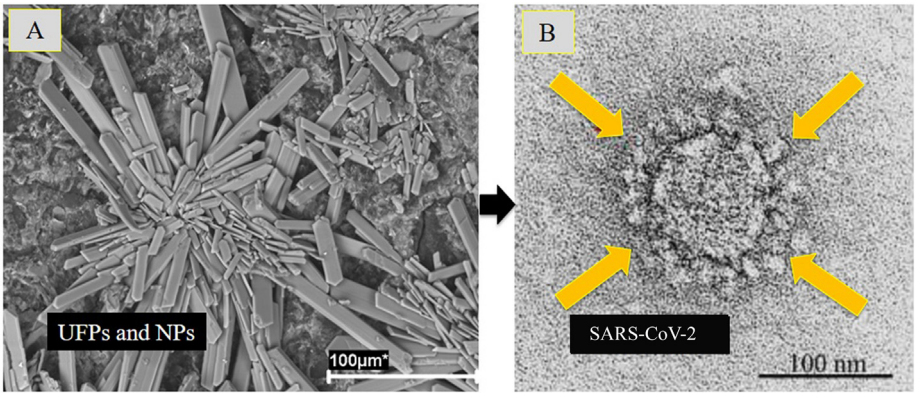

Fig. 3. Representation of the structure of UFPs and NPs (A) and SARS-CoV-2 (B). Source: Image representing the SARS-CoV-2 adapted from Zhu et al. (2020) and Shao et al. (2021), and the representation of UFPs and NPs adapted from Oliveira et al. (2021).

of this virus is in fact ten thousand times thinner than a human hair (Fig. 3B). This small size allows this virus to agglomerate in particles suspended in the air. Microscopic particles that contain viruses can be absorbed into the human body and cause infection by: eating contaminated food and/or water; inhalation of these particles through the airway; and dermal absorption through the skin (Romer et al., 2011; Bakshi, 2020; Leung and Sun, 2020; Silva et al., 2021; Shao et al., 2021).

The greater the intensity of the winds that pass through the structures comprising urban cemeteries, the greater the potential exposure to the population living in the immediate vicinity to viruses, fungi and bacteria liberated through the decay of corpses (Toscan et al., 2020; Cao et al., 2021; Neckel et al. 2021). In addition to being located at some of the highest elevations in the City of Passo Fundo, SARS-CoV-2 cemeteries A, 681 m in elevation, and B, 702 m in elevation (Fig. 4) are also surrounded by areas with the highest population densities of all the cemeteries examined in this study due both to their age and location deep within the urban fabric of Passo Fundo.

Cemeteries A, B and C also exhibit greater potentials for natural ventilation, favoring the dispersion of odors (gases) originated by the decomposition of the high concentration of corpses within the cemeteries and being transported to the neighboring areas by the wind (Ghassoun et al., 2019). Regarding the emission of gases in the vertical urban cemeteries examined in this study, no form of treatment was in place to treat these gaseous emissions. According to (Cao et al., 2021), a comprehensive urban station with instrumentation for monitoring gases and particulates emitted by cemeteries does not yet exist. The development and implementation of such an instrument would be of great use in order to monitor the gaseous contaminants produced by these cemeteries.

According to Neckel et al. (2021) vertical urban cemeteries, generally do not treat gases with biological filters as this would require the incorporation of a plumbing system that funnels gases produced during decomposition through a biological filter. The cemeteries examined in this study were all constructed prior to the availability of such technology, and at a time when gaseous emissions were not necessarily recognized to be harmful. Hino (2015)

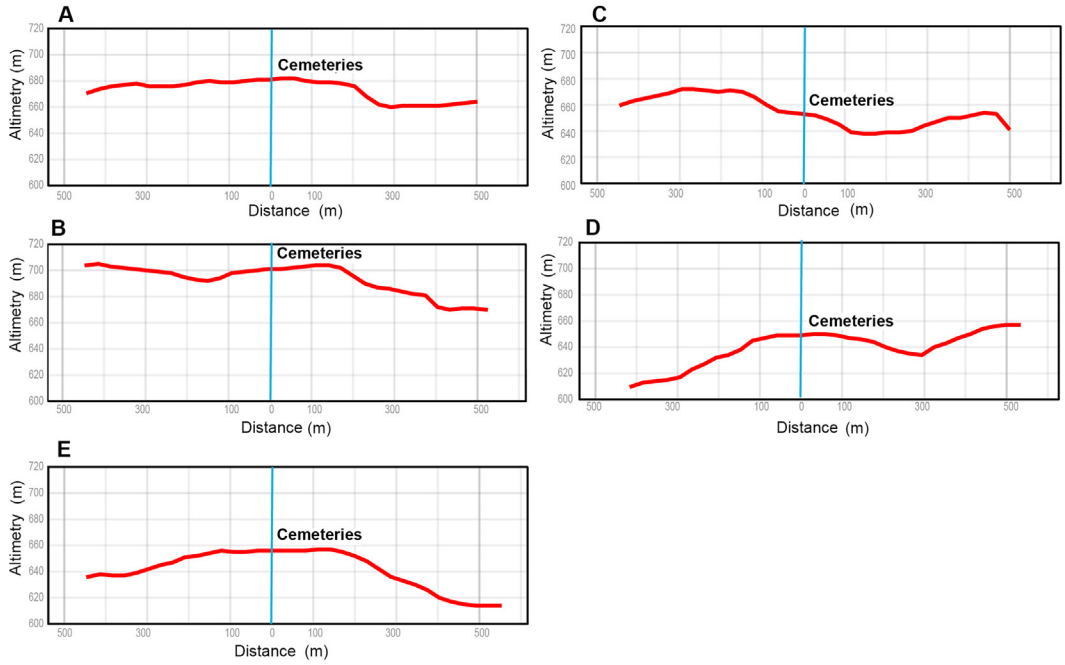

Fig. 4. Altimetric profiles in the period of 2020 of urban cemeteries (point Zero (0)) and their surroundings (radius of 100, 300 and 500 m) in Passo Fundo / RS. Cemeteries: Vera Cruz (A), Petrópolis (B), Ribeiros (C), Jardim da Colina (D) and Roselândia (E).

examines the production and release of gases such as methane (CH_4) during the putrefaction process. As no filters are in place in these urban cemeteries, these gases and particulates are released directly into the open air, traveling directly into adjacent areas via wind action (Hino, 2015). The risk of SARS-CoV-2 viral contamination increases for the population who live in the immediate vicinity of these cemeteries. Although this virus is only viable for a limited time in the ambient environment, depending on environmental conditions, the near constant interment of contaminated corpses in cities undergoing severe outbreaks and large numbers of deaths presents a regular and steady source of fresh virus.

Drageset (2019) highlights the importance of topography when examining the dynamics and intensity of wind speeds on Earth's surface. Comparing our altimetry data with results presented in the published literature, the preeminent influence on the wind intensity of a given area and its ability to transport UFPs and NPs SARS-CoV-2 is altitude (Cao et al., 2021; Oliveira et al., 2021). To reduce some of the negative impacts on the health of the population who reside in close proximity to these urban cemeteries, the authors suggest improving natural ventilation in the area of direct influence of these cemeteries through the implementation and maintenance of green space (Neckel et al., 2020). Evensen et al.

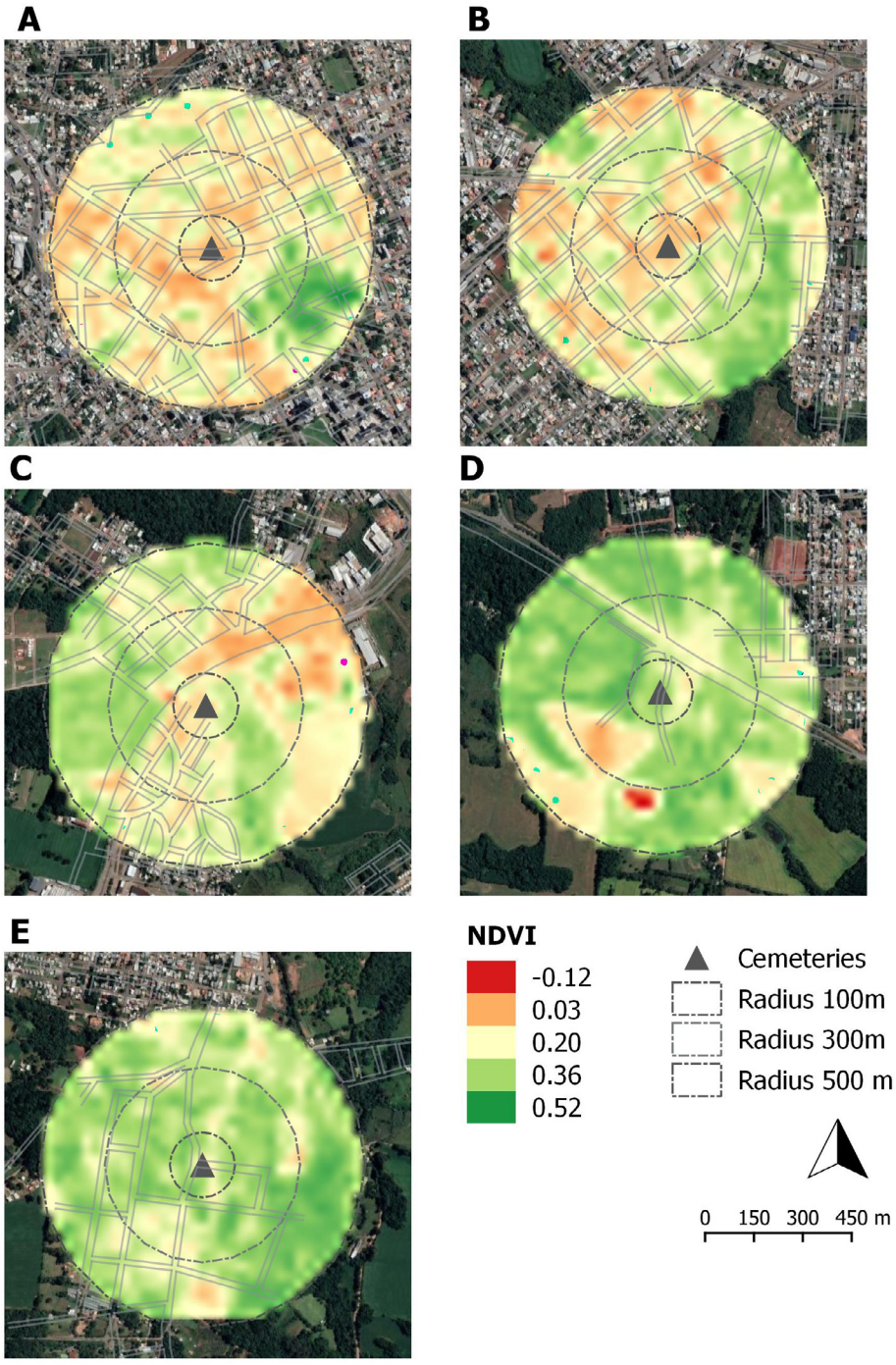

Fig. 5. NDVI maps, using the Landsat 8 satellite from 2013, projected on Google Earth images, applied to urban cemeteries and their surroundings (radii of 100, 300 and 500 m) in Passo Fundo, RS. Cemeteries: Vera Cruz (A), Petrópolis (B), Ribeiros (C), Jardim da Colina (D) and Roselândia (E). Source: Adapted from the IBGE database (2021), USGS (2021), with overlay on Google Earth images (2021).

(2017) and Rae (2021) concluded that it is necessary to implement and maintain green areas in order to alleviate problems with odors and gaseous emissions in cemeteries located within the urban environment.

3.2. Normalized difference vegetation index (NDVI) applied to urban cemeteries and their surrounding areas

The NDVI analysis took into account all forms of vegetation, undergrowth and trees present in the cemeteries of Passo Fundo in relation to their surrounding areas, between 2013 and 2020. Neckel et al. (2020) concluded that decreases in urban vegetation densities were directly correlated with increases in population density and the urbanization of the built environment, which generally suppresses existing urban vegetation. The NDVI analysis is justified, in this study, in order to define the existing levels of urban vegetation through reflectance, to establish a baseline for the application of future public policies which regulate urban projects and allocate the need for trees and other vegetation as an area urbanizes (Guyot et al., 2021).

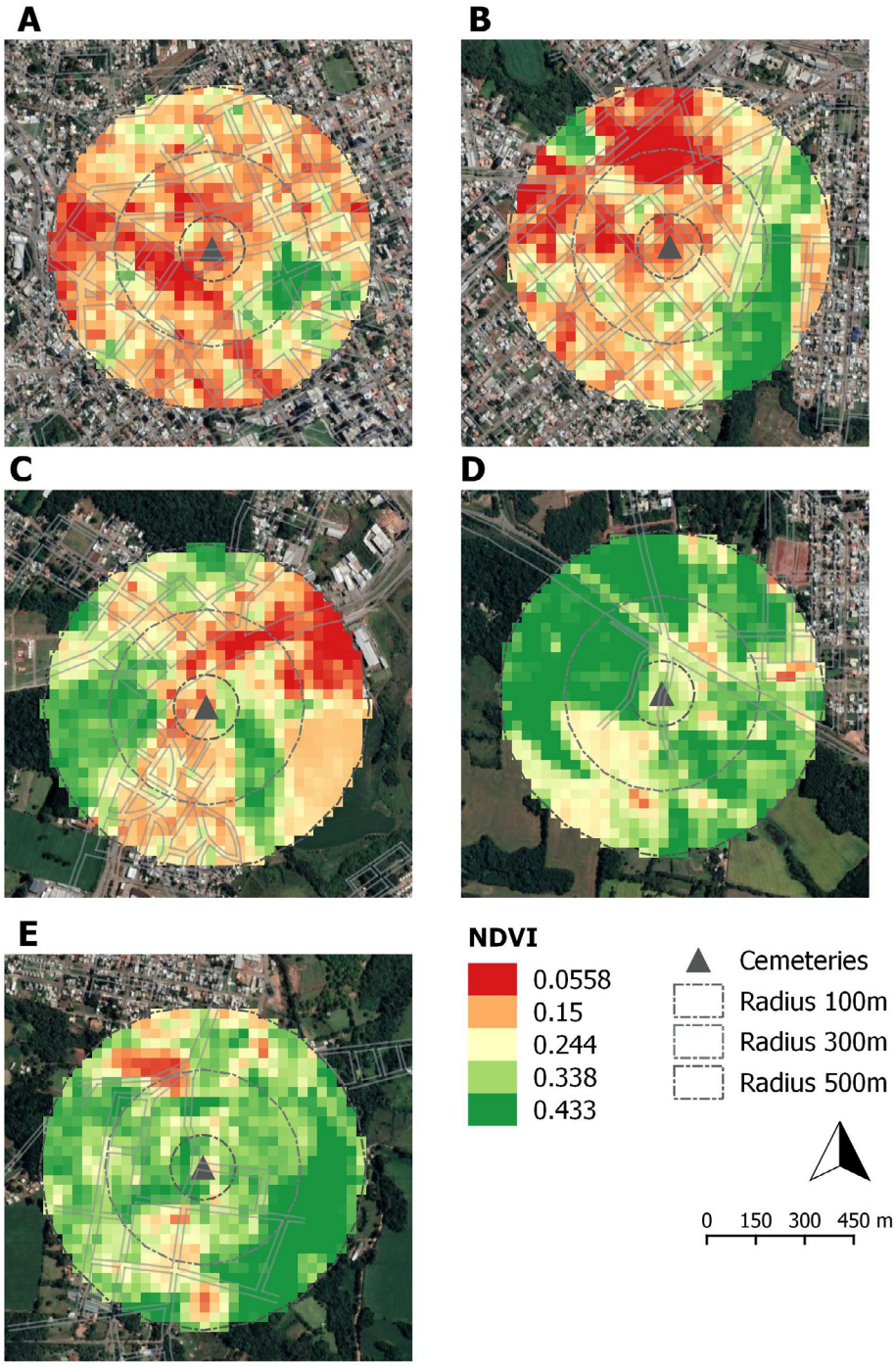

Fig. 6. NDVI maps, using the Landsat 8 satellite of 2020, projected on Google Earth images, applied in urban cemeteries and their surroundings (radii of 100, 300 and 500 m) in Passo Fundo, RS. Cemeteries: Vera Cruz (A), Petrópolis (B), Ribeiros (C), Jardim da Colina (D) and Roselândia (e). Source: Adapted from the IBGE database (2021), USGS (2021), with overlay on Google Earth images (2021).

In the first analysis of the 2013 NDVI data (Fig. 5A, B), the lowest overall vegetative cover was located in cemeteries A and B due to the intense urbanization of their surroundings. Cemeteries C, D and E had higher overall NDVI rates due to the lower levels of urbanization and greater prevalence of vegetation in their vicinities. Neckel et al. (2020), Gavito et al. (2021) and Guyot et al. (2021) highlight the consistent loss of vegetative cover as unregulated urbanization progresses.

Analysis of the 2020 NDVI data set showed a marked decrease in NDVI due to urbanization for cemeteries A and B (Fig. 6). Cemetery C displayed a moderate NDVI index, whereas cemeteries D and E displayed the highest overall NDVI values. The largest area of low NDVI in the vicinity of cemetery E resulted from the implementation of a new housing subdivision. The presence of vegetation around cemeteries is very beneficial in terms of sanitation and hygiene as the vegetation serves as an air purifying agent in addition to a physical barrier to the transport of UFPs and NPs through the air.

Cemeteries A and B exhibit a more uniform NDVI that is closer to zero (0) due to the high urbanization rates in the urban fabric of the city. In the profile of cemetery A (Fig. 7), the highest NDVI rating is due to a fragment of forest known as Banhado da Vergueiro Park. This highlights the findings of Neckel et al. (2020) and Toscan et al. (2020) who highlighted the importance of the existence of urban parks as an effort to raise NDVI and improve the health and quality of life for the local population.

Compared to cemetery A, cemetery B is surrounded by a less uniform urban fabric, with parcels of undeveloped land covered in vegetation. In addition, cemetery B is located in close proximity to the Passo Fundo River. Fig. 7 shows that cemeteries C, D and E all have very low vegetative cover in close proximity to their geographical centers as compared to distances further out, allowing for virtually unimpeded wind flow and potential contaminant spread SARS-CoV-2. It is therefore necessary to carry out LST studies to better understand urban dynamics based on the consequences of altimetry and variations in vegetation density which can influence the transport of nanoparticles through winds (Toscan et al., 2020).

3.3. Land surface temperature (LST) of urban cemeteries and their surrounding areas

Figs. 8 and 9 display the LST data analyzed for 2013 and 2020, respectively. A significant difference is shown between the two data sets for all cemeteries analyzed. Cemeteries A and B display higher overall LST values more uniformly dispersed throughout as opposed to locations with fragments of vegetative cover or Permanent Preservation Areas (PPAs) (Fig. 8A, B). He et al. (2020) similarly showed that areas in the vicinity of water resources and PPAs exhibited lower overall terrestrial temperatures (cemetery B).

Cemeteries C, D and E, each located on the outskirts of the current city, remain in close proximity to agricultural activity on the urban border, resulting in decreasing uniformity of LST values from C to D to E (Fig. 8C, D, E). As urbanization progresses in these vicinities, we expect the LST graphs of cemeteries C, D and E to more closely resemble those of cemeteries A and B. Terrestrial temperatures generally increase as the built environment expands, an effect known as the heat island effect. One potential solution to this would be the implementation of regulations accompanying a city's growth that require the preservation and incorporation of green spaces, thereby mitigating negative health impacts caused by increased temperatures (Duncan et al., 2019; Chi et al., 2020; Sayão et al., 2020; Shi et al., 2021).

Fig. 9 displays the LST data analysis from the 2020 data set. Again, cemeteries A and B displayed the most uniform yet higher LST values when compared to 2013, with fragments of vegetation and PPAs close to water resources displaying lower temperatures (Fig. 9A, B). Cemetery C displayed the largest overall increase in LST throughout the area between 2013 and 2020 (Fig. 9C) whereas cemetery D displayed highly concentrated yet significant LST increase mostly in the SW perimeter (Fig. 9D). This increase in LSTs in both cemeteries C and D are attributed to a decrease in areas with agricultural cultivation and an increase in development in both of these locations in relation to 2013. Cemetery E also displays this trend, although to a lesser degree (Fig. 9E).

Figs. 8 and 9 show that the internal cores of the cemeteries in close proximity to the center exhibit lower overall rises in LST, remaining somewhat static between 2013 and 2020. As outlined

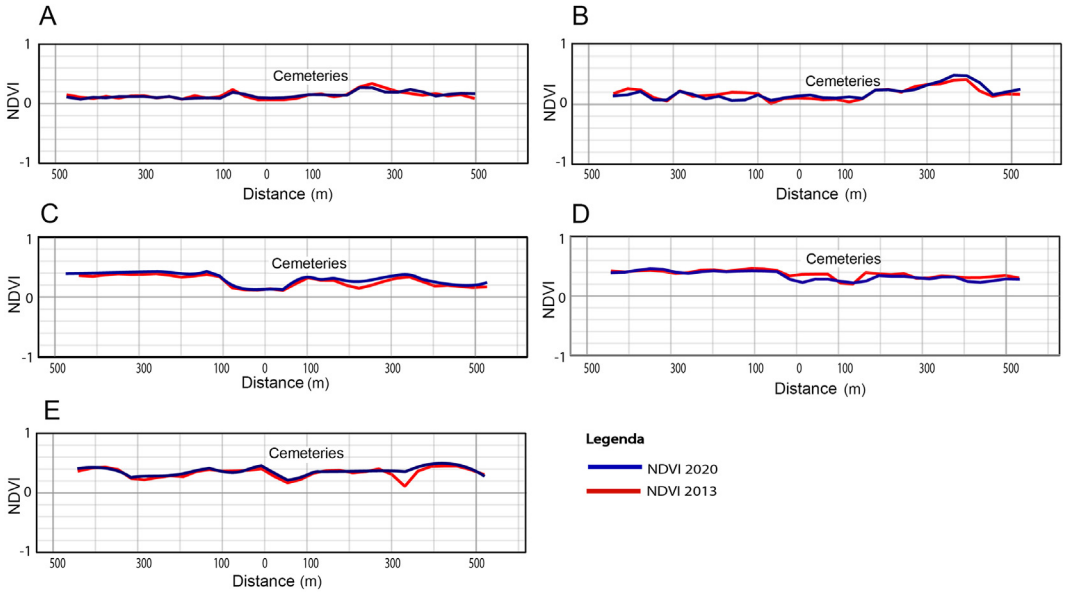

Fig. 7. Comparison of 2013 and 2020 NDVI profiles of Passo Fundo's five urban cemeteries (zero point (0)) and the surrounding (radii of 100, 300 and 500 m). Cemeteries: Vera Cruz (A), Petrópolis (B), Ribeiros (C), Jardim da Colina (D) and Roselândia (E).

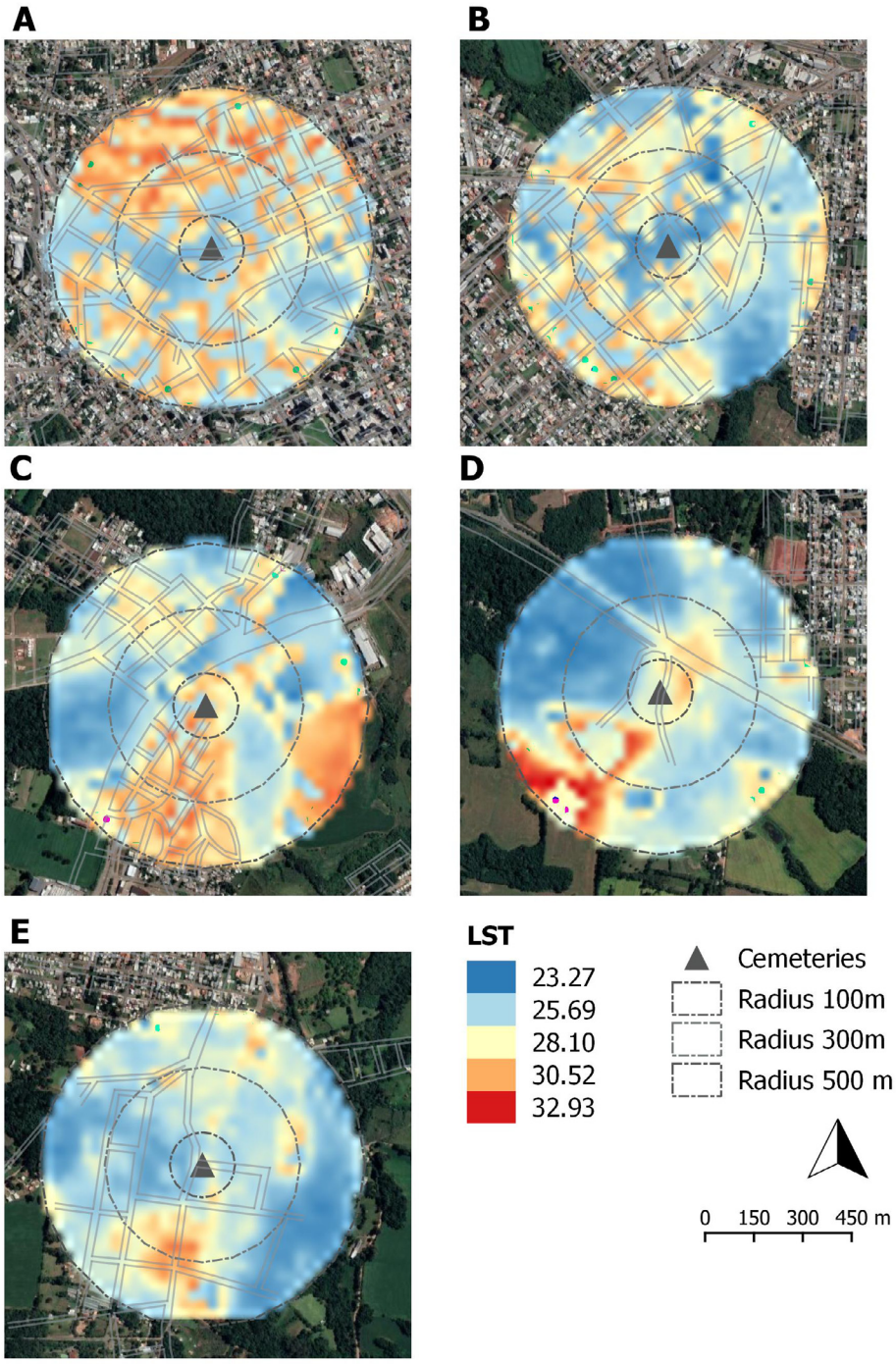

Fig. 8. LST maps, using the Landsat 8 satellite from 2013, projected on Google Earth images, applied to urban cemeteries and their surroundings (radii of 100, 300 and 500 m) in Passo Fundo, RS. Cemeteries: Vera Cruz (A), Petrópolis (B), Ribeiros (C), Jardim da Colina (D) and Roselândia (E). Source: Adapted from the IBGE database (2021), USGS (2021), with overlay on Google Earth images (2021).

in Abia et al. (2019) and Toscan et al. (2020), this decrease in surface temperature of urban cemeteries occurs because there are no tall structures to block the wind, only tombs, vaults and pits in which the deceased are interred. This makes it possible for winds to circulate easily and intensely throughout the cemetery, promoting further cooling of the earth's surface in these areas (Prangnell and Mcgowan, 2009; Toscan et al., 2020; Wu et al., 2020). This dynamic of cooling through convection is quite evident in the urban cemeteries of Passo Fundo. The worrisome aspect of this comes to light with the current pandemic, that these unimpeded winds may potentially carry viral particles derived from the off gassing of the recently deceased SARS-CoV-2 along with other contaminants present in the structures off-site by the wind.

In this context, starting from the zero point (0) that corresponds to the geographic center of each of the urban cemeteries of Passo Fundo, the following mean daily summer LSTs were recorded for 2013: 25.1 °C in cemetery A, 24.3 °C (B), 25.7 °C (C), 27.3 °C (D) and 23.6 °C (E) (Fig. 10). By 2020, these mean daily summer LSTs had increased to: 28.2 °C in cemetery A, 28.5 °C (B) and 28.6 °C (C) (Fig. 10). Temperatures outside of the cemeteries' boundaries were consistently 3 °C above those recorded at each cemetery's zero point. For Adulkongkaew et al. (2020) and Alexander (2021),

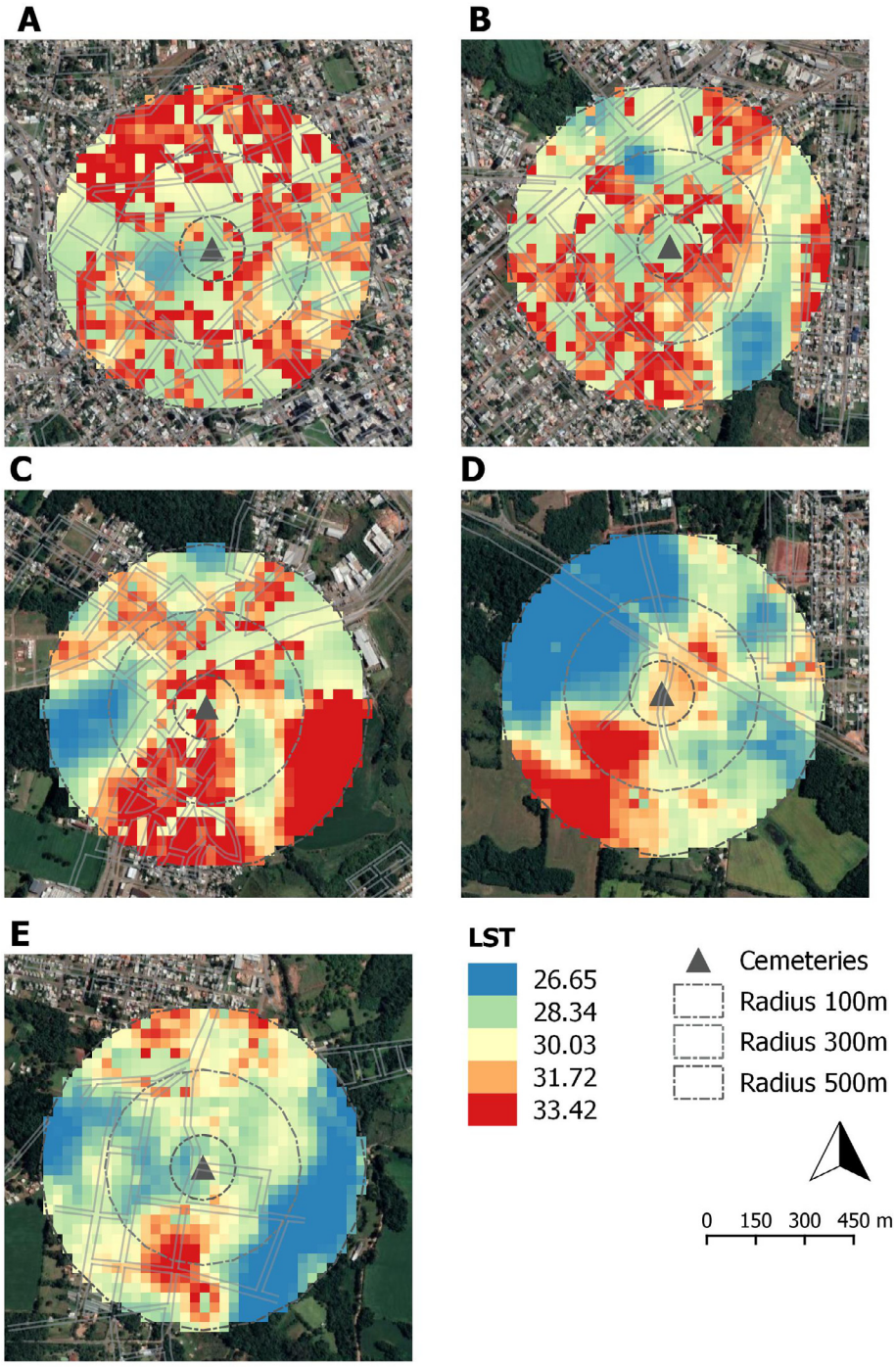

Fig. 9. LST maps, using the Landsat 8 satellite from 2020, projected on Google Earth images, applied to urban cemeteries and their surroundings (radii of 100, 300 and 500 m) in Passo Fundo, RS. Cemeteries: Vera Cruz (A), Petrópolis (B), Ribeiros (C), Jardim da Colina (D) and Roselândia (E). Source: Adapted from the IBGE database (2021), USGS (2021), with overlay on Google Earth images (2021).

the difference in variation of the measured LSTs is due to the heterogeneity of the areas themselves, as different materials have different reflectance properties, and therefore, different heating capacities. The majority of the construction materials that make up the tombs within the cemetery are of rather uniform composition.

Fig. 10 highlights the significant rises and drops in the LST of the three cemeteries (A, B and C) that are surrounded by the most development overall. This trend is not displayed for cemeteries D and E, the surroundings of which are far less urbanized. Highly urbanized areas that contain many buildings of varying size that block convection near the ground and paved, impervious areas that re-radiate heat are typically higher in surface temperature than more natural areas with ample vegetation and pervious ground. Fig. 10 demonstrates this principle well.

These results agree with the findings of Duncan et al. (2019), Alexander (2020), Chi et al. (2020), Guha et al. (2020), Toscan et al. (2020) and Shi et al. (2021) which highlight the fundamental

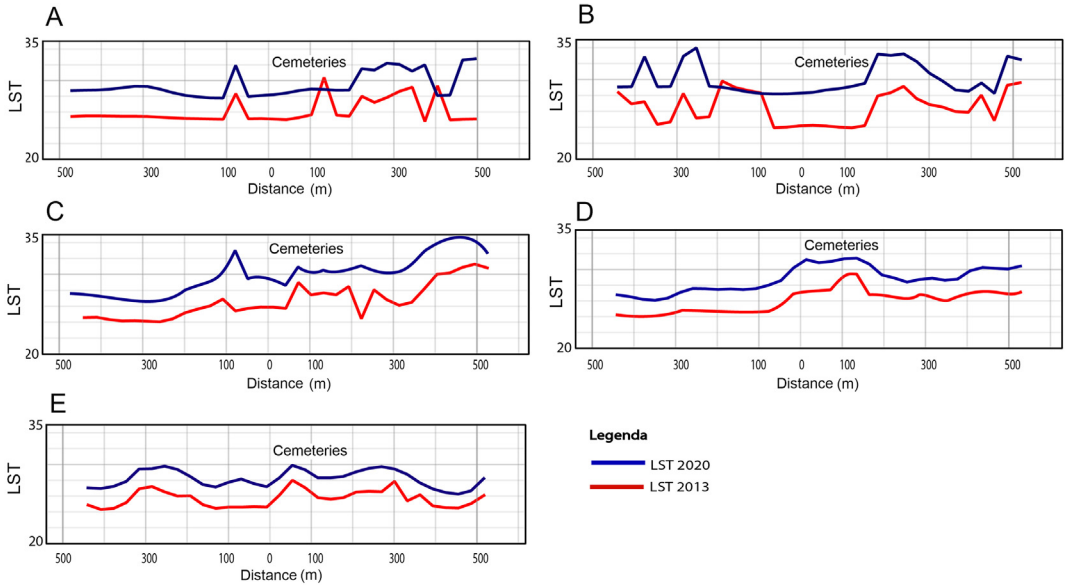

Fig. 10. LST profiles in the period 2013 and 2020 of urban cemeteries (point Zero (0)) and their surroundings (radii of 100, 300 and 500 m) in Passo Fundo, RS. Cemeteries: Vera Cruz (A), Petrópolis (B), Ribeiros (C), Jardim da Colina (D) and Roselândia (E).

Table 2
Analysis of Pearson's correlation of significance in relation to altimetry, NDVI and LST in the urban cemeteries of Passo Fundo and their surroundings.

Variables	Probability	ALT (2020)	NDVI 2013	NDVI 2020	LST 2013	LST 2020
1. ALT	Pearson's r	–	–	–	–	–
	p-value	–	–	–	–	–
2. NDVI 2013	Pearson's r	−0.37327	–	–	–	–
	p-value	0.00002	–	–	–	–
3. NDVI 2020	Pearson's r	−0.51983	0.80860	–	–	–
	p-value	5.21897e−10	4.09971e−30	–	–	–
4. LST 2013	Pearson's r	−0.00937	−0.14918	−0.21445	–	–
	p-value	0.91743	0.09682	0.01633	–	–
5. LST 2020	Pearson's r	0.27676	−0.40650	−0.47088	0.62090	–
	p-value	0.00178	2.55247e−6	2.99495e−8	1.12438e−14	–

importance of urban studies that relate factors such as the influence of winds, degree of vegetative cover, altimetry and LST to fully understanding the effects of urbanization.

3.4. Correlation applied in altimetry, NDVI and LST

The use of the Pearson correlation coefficient (Edelmann et al., 2021), allowed for the distribution of variables whose results can be both positive and negative in a random and finite way. Correlation analysis was performed to further the understanding and quantification of dependence strength between variables, with the goal of understanding absolute values of differences, with certain variables expressed in measures. The study variables were classified as: ALT 2020 (altimetry), NDVI 2013 and NDVI 2020, LST 2013 and LST 2020. Using Pearson's correlation, it became possible to analyze the similarity between the variables that show significance, assuming values between −1 and 1, which make it possible to analyze the relationship between significant variables (Baak et al., 2020). The correlation (r) between two variables ($x + y = xy$) in a linear fashion consists of a pure number (−1 to +1), which can vary in certain correlation patterns according to the type of significance, which consists of values of the result of the correlation of the variables (Bermudez-Edo et al., 2018; Edelmann et al., 2021).

This study yielded weak correlations between altimetry (ALT) (2020) and NDVI (2013 and 2020), of negative characteristic; indicating that, as altimetry increases, the NDVI value decreases. This makes ALT 2020 insignificant for the analysis as it presents only a temporal scenario. The NDVI (2013 and 2020) and the LST (2013 and 2020) have moderate and negative significance, with a value of "r" equal to −0.40 and −0.47, respectively. This was expected according to the specialized bibliography (Baak et al., 2020; Edelmann et al., 2021). Altimetry and LST remain significant, however yield a weak correlation value of "r" of 0.27 (Table 2).

As seen in Fig. 11, the dispersion between NDVI and LST show the concentration of the data and the correlation between the two variables, with the index "r" having a moderate correlation value of −0.47. When analyzing the correlation between altimetry and LST, there is a dispersion of the data, demonstrating that the sampling error is greater in this relationship, thus, there are other factors that influence the increase in the reflectance temperature of the Earth's surface. This reinforces the LST 2013 variable in Pearson's correlation, with a significant "r" value of 0.277.

Pearson's correlation made it possible to identify the degree of significance between variables. It is also possible to identify p- values, which determine significance when less than 0.05 (Bermudez-Edo et al., 2018; Edelmann et al., 2021). According to Table 3, for the radius zero, p-value was significant in the

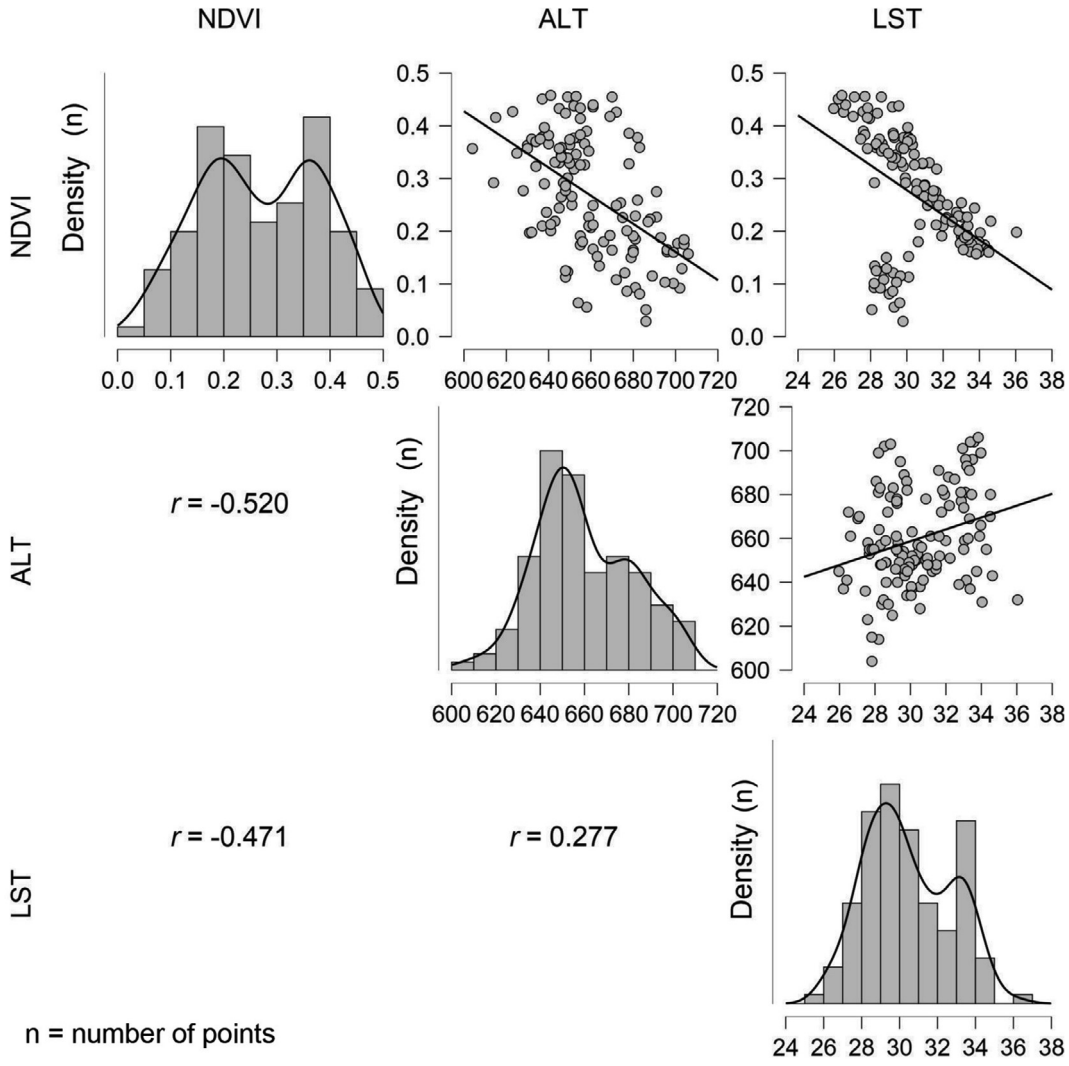

Fig. 11. Scatter plots of ALT 2020, NDVI 2013, NDVI 2020, LST 2013 and LST 2020 variables.

correlation between altimetry and NVDI, yielding a value of 0.028 for the year 2013 and 0.027 for the year 2020, respectively. Both variables presented moderate correlations, with an "r" index equal to −0.60.

An analysis radius of 100 m from the central geographic point of the urban cemeteries examined yielded a significant p-value in three correlations. Altimetry and NVDI (2013 and 2020) showed a moderate degree of correlation with values of −0.56 and −0.65, respectively in the cemeteries with the lowest rates of urbanization (C, D and E) (Table 2). Further correlations were found within a 300 m radius. LST 2020 and NDVI 2020 displayed a moderate degree of correlation with a value of 0.65. Of the 500 m radii, significant p-value correlation was found among three variables: ALT and NDVI 2020, LST 2020 and ALT, and LST 2020 and NDVI 2020.

Pearson's correlation demonstrated that altimetry (2020) and NVDI (2013), while presenting moderate indices, allow us to relate that, the higher the altitude, the lower the density of vegetation. It is understood that this result cannot be considered as a standard, since the areas with the highest urban density is located in the area with the highest altitude (around cemeteries A and B). Highly urbanized areas contain little vegetation and thus present few physical barriers to the potential movement of SARS-CoV-2 virus particles.

These results in Pearson's correlation (Table 3), show that altimetry (2020) and NDVI 2020, LST 2020 and altimetry (2020), and LST2020 and NDVI 2020 all have relationships capable of influencing urban dynamics. This supports the conclusions of Toscan et al. (2020), who state that altimetry, NDVI and LST should be considered in urban studies, especially given the wealth of data freely available through satellite images. What makes it possible to understand the relationships of altitude, vegetation and temperature, that they exert on cemeteries and in their surrounding area, with direct influences, being subject to the proliferation of contaminants, released during the process of decomposition of buried bodies, thus supposes a greater possibility of contamination by SARS-CoV-2 as a result of urban cemeteries, not only considering the city of Passo Fundo, but also a concern on a global scale.

Table 3
Analysis of Pearson's correlation of significance in relation to altimetry, NDVI and LST in the urban cemeteries of Passo Fundo and their surroundings, within radii of 100, 300 and 500 m.

Pearson's correlation analysis for radius 0 (point 0) - of the cemeteries analyzed						
Variables	Probability	ALT (2020)	NDVI 2013	NDVI 2020	LST 2013	LST 2020
1. ALT	Pearson's r	–	–	–	–	–
	p-value	–	–	–	–	–
2. NDVI 2013	Pearson's r	−0.60639	–	–	–	–
	p-value	0.02801	–	–	–	–
3. NDVI 2020	Pearson's r	−0.60832	0.97037	–	–	–
	p-value	0.02738	3.95003e−8	–	–	–
4. LST 2013	Pearson's r	−0.52087	0.44625	0.35307	–	–
	p-value	0.06798	0.12638	0.23667	–	–
5. LST 2020	Pearson's r	−0.28225	−0.05209	−0.17058	0.33603	–
	p-value	0.35013	0.86580	0.57740	0.26164	–
Pearson's correlation analysis for radius of 100 m						
Variables	Probability	ALT (2020)	NDVI 2013	NDVI 2020	LST 2013	LST 2020
1. ALT	Pearson's r	–	–	–	–	–
	p-value	–	–	–	–	–
2. NDVI 2013	Pearson's r	−0.56724	–	–	–	–
	p-value	0.00014	–	–	–	–
3. NDVI 2020	Pearson's r	−0.65499	0.94391	–	–	–
	p-value	4.52276e−6	7.01996e−20	–	–	–
4. LST 2013	Pearson's r	−0.00405	−0.10471	−0.20789	–	–
	p-value	0.98021	0.52020	0.19801	–	–
5. LST 2020	Pearson's r	0.31856	−0.31103	−0.44596	0.65105	–
	p-value	0.04513	0.05076	0.00392	5.39250e−6	–
Pearson's correlation analysis for radius of 300 m						
Variables	Probability	ALT (2020)	NDVI 2013	NDVI 2020	LST 2013	LST 2020
1. ALT	Pearson's r	–	–	–	–	–
	p-value	–	–	–	–	–
2. NDVI 2013	Pearson's r	−0.20797	–	–	–	–
	p-value	0.02801	–	–	–	–
3. NDVI 2020	Pearson's r	−0.53420	0.75316	–	–	–
	p-value	0.00038	2.05578e−8	–	–	–
4. LST 2013	Pearson's r	0.13953	−0.25896	−0.40665	–	–
	p-value	0.39050	0.10663	0.00922	–	–
5. LST 2020	Pearson's r	0.42566	−0.57995	−0.68904	0.64929	–
	p-value	0.00617	0.00009	8.83564e−7	5.82910e−6	–
Pearson's correlation analysis for radius of 500 m						
Variables	Probability	ALT (2020)	NDVI 2013	NDVI 2020	LST 2013	LST 2020
1. ALT	Pearson's r	–	–	–	–	–
	p-value	–	–	–	–	–
2. NDVI 2013	Pearson's r	−0.26561	–	–	–	–
	p-value	0.09762	–	–	–	–
3. NDVI 2020	Pearson's r	−0.36930	0.70320	–	–	–
	p-value	0.01902	4.19238e−7	–	–	–
4. LST 2013	Pearson's r	−0.12974	−0.27880	−0.21369	–	–
	p-value	0.42492	0.08149	0.18551	–	–
5. LST 2020	Pearson's r	0.14961	−0.48977	−0.42425	0.57926	–
	p-value	0.35685	0.00134	0.00637	0.00009	–

4. Conclusions

The manuscript highlights the analysis of the reflectance of altimetry, NDVI and LST in urban cemeteries in a mid-sized city in southern Brazil. The relationship between certain physical dynamics may be contributing to greater spread of active SARS-CoV-2 viral particles among areas of dense residential housing in global scale. This study recommends future research on the monitoring of air quality in urban cemeteries, considering the physical influences of altimetry, surface temperature and vegetation. This study examined two cemeteries (A and B) built in the 20th century at some of the highest elevations in the city and now surrounded on all sides by dense residential neighborhoods with little natural vegetation pose a greater risk of potentially spreading infectious particles or contaminants than those at lower elevations and/or on the outskirts of town not surrounded by dense urbanization (C, D and E). The system was investigated using the dynamics of altimetry, NDVI and LST in urban environments highlight the possibility of contaminants being released to the surrounding environment in urban cemeteries commonly utilized in many countries of the world. Any burial practice in which a corpse is allowed to both decompose without the use of embalming agents and remains above ground or is placed in a tomb or niche that is not air tight, has the potential to shed and spread particles and fluids as it decays. This is of especially great concern during world-wide pandemics in which the rate of entombment is both high and steady and the agent causing the disease is readily shed by those infected with it after death.

We recommend to initiate immediate air monitoring around all five cemeteries examined in this study (A, B, C, D and E) in order to determine the presence of any potential disease causing agents, including the SARS-CoV-2 virus. It is also recommended that the City of Passo Fundo establishes guidelines and/or regulations for all future construction projects in order to raise the levels of

resulting NDVI once the project is complete, thus minimizing LST and enhancing atmospheric filtration to enable a higher quality of life for the resident population.

The results of this study point to the ease of proliferation of SARS-CoV-2 virus in relation to the physical dynamics of the environment. Thus, it is suggested that future research need to focus on assessing the possible proliferation of SARS-CoV-2 virus in urban cemeteries.

Declaration of Competing Interest

The authors declare that they have no known competing financial interests or personal relationships that could have appeared to influence the work reported in this paper.

Acknowledgments

We thank the Guest Editor and three anonymous referees for their constructive comments and suggestions which improved this paper. The authors are grateful to the USGS and NASA for providing the processed images of the Landsat 8 satellite. We also wish to thank the Center for Studies and Research on Urban Mobility (NEPMOUR / IMED). We thank the Brazilian National Council for Scientific and Technological Development (CNPq) linked to the Ministry of Science, Technology, Innovations and Communications for the financial incentive in this study (Process: 426453/2018-2).

References

Abia, A.L.K., Alisoltani, A., Ubomba-Jaswa, E., Dippenaar, M.A., 2019. Microbial life beyond the grave: 16s rrna gene-based metagenomic analysis of bacteria diversity and their functional profiles in cemetery environments. Sci. Total Environ. 655, 831–841.

Adulkongkaew, T., Satapanajaru, T., Charoenhirunyingyos, S., Singhirunnusorn, W., 2020. Effect of land cover composition and building configuration on land surface temperature in an urban-sprawl city, case study in Bangkok Metropolitan Area, Thailand. Heliyon 6 (8), 1–13.

Ahmed, T., Singh, D., 2020. Probability density functions based classification of MODIS NDVI time series data and monitoring of vegetation growth cycle. Adv. Space Res. 66 (4), 873–886.

Alexander, C., 2020. Normalised difference spectral indices and urban land cover as indicators of land surface temperature (LST). Int. J. Appl. Earth Obs. Geoinf. 86, 102013.

Alexander, C., 2021. Influence of the proportion, height and proximity of vegetation and buildings on urban land surface temperature. Int. J. Appl. Earth Obs. Geoinf. 95, 1–12.

Anand, U., Adelodun, B., Pivato, A., Suresh, S., Indari, O., Jakhmola, S., Jha, H.C., Jha, P. K., Tripathi, V., Maria, F.D., 2021. A review of the presence of SARS-CoV-2 RNA in wastewater and airborne particulates and its use for virus spreading surveillance. Environ. Res. 196, 110929.

Baak, M., Koopman, R., Snoek, H., Klous, S., 2020. A new correlation coefficient between categorical, ordinal and interval variables with Pearson characteristics. Comput. Stat. Data Anal. 152, 107043.

Balta, J.Y., Blom, G., Davidson, A., Perrault, K., Cryan, J.F., O'mahony, S.M., Cassella, J. P., 2020. Developing a quantitative method to assess the decomposition of embalmed human cadavers. Forensic Chem. 18, 100235.

Bakshi, M.S., 2020. Impact of nanomaterials on ecosystems: mechanistic aspects in vivo. Environ. Res. 182, 109099.

Blanar, K., Prada-Tiedemann, P.A., 2020. Characterization of the volatile odor profile from larval masses in a field decomposition setting. Forensic Chem. 21, 100288.

Barcelo, D., 2020. An environmental and health perspective for COVID-19 outbreak: meteorology and air quality influence, sewage epidemiology indicator, hospitals disinfection, drug therapies and recommendations. J. Environ. Chem. Eng. 8, (4) 104006.

Bermudez-Edo, M., Barnaghi, P., Moessner, K., 2018. Analysing real world data streams with spatio-temporal correlations: entropy vs. Pearson correlation. Autom. Constr. 88, 87–100.

Bonatti, M., Lana, M.A., D'agostini, L.R., de Vasconcelos, A.C.F., Sieber, S., Eufemia, L., da Silva-Rosa, T., Schlindwein, S.L., 2019. Social representations of climate change and climate adaptation plans in southern Brazil: challenges of genuine participation. Urban Clim. 29, 100496.

Calmon, M., 2020. Considerations of coronavirus (COVID-19) impact and the management of the dead in Brazil. Forensic Sci. Int., 100110

Cao, Y., Shao, L., Jones, T., Oliveira, M.L.S., Ge, S., Feng, X., Silva, L.F.O., Bérubé, K., 2021. Multiple relationships between aerosol and COVID-19: a framework for global studies. Gondwana Res. 93, 243–251.

Cazenave, A., 2019. Satellite Altimetry. Encyclopedia of Ocean Sciences (Third Edition) 5, 397–401.

Chatterjee, R.S., Singh, N., Thapa, S., Sharma, D., Kumar, D., 2017. Retrieval of land surface temperature (LST) from landsat TM6 and TIRS data by single channel radiative transfer algorithm using satellite and ground-based inputs. Int. J. Appl. Earth Obs. Geoinf. 58, 264–277.

Chemura, A., Mutanga, O., Dube, T., 2017. Integrating age in the detection and mapping of incongruous patches in coffee (Coffea arabica) plantations using multi-temporal Landsat 8 NDVI anomalies. Int. J. Appl. Earth Obs. Geoinf. 57, 1–13.

Chi, Y., Sun, J., Sun, Y., Liu, S., Fu, Z., 2020. Multi-temporal characterization of land surface temperature and its relationships with normalized difference vegetation index and soil moisture content in the Yellow River Delta, China. Glob. Ecol. Conserv. 23, 01092.

Cilek, M.U., Cilek, A., 2021. Analyses of land surface temperature (LST) variability among local climate zones (LCZs) comparing Landsat-8 and ENVI-met model data. Sustain. Cities Soc., 102877–102881

Costa, C.A.G., Teixeira, A.dos.S., Andrade, E.M.de., Lucena, A.M.P.de., Castro, M.A.H. de, 2010. Analysis of vegetation influence on altimetry of SRTM data in watersheds in the semiarid region. Rev. Cienc. Agron. 41 (2), 222–230.

Costa, L., Nunes, L., Ampatzidis, Y., 2020. A new visible band index (vNDVI) for estimating NDVI values on RGB images utilizing genetic algorithms. Comput. Electron. Agric. 172, 105334.

Das, M., Das, A., 2020. Assessing the relationship between local climatic zones (LCZs) and land surface temperature (LST) – a case study of Sriniketan-Santiniketan Planning Area (SSPA), West Bengal. India. Urban Clim. 32, 100591.

Drageset, A., 2019. The Hereid cemetery: relational agency and topography within the iron age mortuary landscape of Hardanger, Western Norway. J. Hist. Geogr. 66, 81–92.

Duarte, A.L., Schneider, I.L., Artaxo, P., Oliveira, M.L.S., 2021. Spatiotemporal assessment of particulate matter (PM10 and PM2.5) and ozone in a Caribbean urban coastal city. Geosci. Front. 101168, 1–9.

Duncan, J.M.A., Boruff, B., Saunders, A., Sun, Q., Hurley, J., Amati, M., 2019. Turning down the heat: an enhanced understanding of the relationship between urban vegetation and surface temperature at the city scale. Sci. Total Environ. 656, 118–128.

Edelmann, D., Móri, T.F., Székely, G.J., 2021. On relationships between the Pearson and the distance correlation coefficients. Stat. Probab. Lett. 169, 108960.

Embrapa (Brazilian Agricultural Research Corporation), 2021. Climate of Passo Fundo in Brazil. Technical Reports. https://www.embrapa.br/busca-de-publicacoes/-/publicacao/939638/base-de-dados-climaticos.

Evensen, K.H., Nordh, H., Skaar, M., 2017. Everyday use of urban cemeteries: a Norwegian case study. Landsc. Urban Plan. 159, 76–84.

Gasparin, F., Cravatte, S., Greiner, E., Perruche, C., Hamon, M., Van Gennip, S., Lellouche, J.M., 2021. Excessive productivity and heat content in tropical Pacific analyses: disentangling the effects of in situ and altimetry assimilation. Ocean Model. 160, 101768.

Gavito, M.E., Paz, H., Barragán, F., Siddique, I., Arreola-Villa, F., Pineda-García, F., Balvanera, P., 2021. Indicators of integrative recovery of vegetation, soil and microclimate in successional fields of a tropical dry forest. For. Ecol. Manag. 479, 118526.

Ghassoun, Y., Löwner, M.O., Weber, S., 2019. Wind direction related parameters improve the performance of a land use regression model for ultrafine particles. Atmos. Pollut. Res. 10 (4), 1180–1189.

Gozdowski, D., Stępień, M., Panek, E., Varghese, J., Bodecka, E., Rozbicki, J., Samborski, S., 2020. Comparison of winter wheat NDVI data derived from Landsat 8 and active optical sensor at field scale. Remote Sens. Appl. Soc. Environ. 20, 100409.

Guha, S., Govil, H., Gill, N., Dey, A., 2020. A long-term seasonal analysis on the relationship between LST and NDBI using Landsat data. Quat. Int., 1–36

Guyot, M., Araldi, A., Fusco, G., Thomas, I., 2021. The urban form of Brussels from the street perspective: the role of vegetation in the definition of the urban fabric. Landsc. Urban Plan. 205, 1–13.

He, H., He, D., Jin, J., Smits, K.M., Dyck, M., Wu, Q., Si, B., Lv, J., 2020. Room for improvement: a review and evaluation of 24 soil thermal conductivity parameterization schemes commonly used in land-surface, hydrological, and soil-vegetation-atmosphere transfer models. Earth-Sci. Rev. 211, 103419.

Herbst, K.W., Beckers, G.M.A., Harper, L., Bägli, D.J., Nieuwhof-Leppink, A.J., Kaefer, M., Fossum, M., Kalfa, N., 2020. Don't be mean, be above average: understanding data distribution and descriptive statistics. J. Pediatr. Urol. 16 (5), 712.

Hino, T.M., 2015. The necrochorume and the environmental management of cemeteries. Esp. On-line IPOG 1 (10).

IBGE (Brazilian Institute of Geography and Statistics), 2021. Brazilian Institute of Geography and Statistics. Demographic Data of 2021 – Brazil. https://cidades.ibge.gov.br/.

Jansi, R.S., Khusro, A., Agastian, P., Alfarhan, A., Al-Dhabi, N.A., Arasu, M.V., Rajagopal, R., Barcelo, D., Al-Tamimi, A., 2021. Emerging paradigms of viral diseases and paramount role of natural resources as antiviral agents. Sci. Total Environ. 759, 143539.

King, A.P., Eckersley, R.J., 2019. Descriptive Statistics III: roc analysis. Statist. Biomed. Eng. Sci., 57–69

Lalwani, A., Gautam, S., 2021. Lockdown during COVID-19 pandemic: a case study from Indian cities shows insignificant effects on urban air quality. Geosci. Front., 101284

Leung, W.W.F., Sun, Q.Q., 2020. Electrostatic charged nanofiber filter for filtering airborne novel coronavirus (COVID-19) and nano-aerosols. Sep. Purif. Technol. 250, 17.

Li, H., Zhou, Y., Jia, G., Zhao, K., Dong, J., 2021. Quantifying the response of surface urban heat island to urbanization using the annual temperature cycle model. Geosci. Front., 101141

Maroni, D., Cardoso, G.T., Neckel, A., Maculan, L.S., Oliveira, M.L.S., Bodah, E.T., Bodah, B.W., Santosh, M., 2021. Land surface temperature and vegetation index as a proxy to microclimate. J. Environ. Chem. Eng. 9, (4) 105796.

Mikszewski, A., Stabile, L., Buonanno, G., Morawska, L., 2021. The airborne contagiousness of respiratory viruses: a comparative analysis and implications for mitigation. Geosci. Front., 101285

Moreno, R., Ojeda, N., Azócar, J., Venegas, C., Inostroza, L., 2020. Application of NDVI for identify potentiality of the urban forest for the design of a green corridors system in intermediary cities of Latin America: case study, Temuco, Chile. Urban For. Urban Green. 55, 126821.

Moreno, T., Gibbons, W., 2021. Aerosol transmission of human pathogens: from miasmata to modern viral pandemics and their preservation potential in the anthropocene record. Geosci. Front., 101282

Nascimento, C.M., Mendes, W.de.S., Silvero, N.E.Q., Poppiel, R.R., Sayão, V.M., Dotto, A.C., Santos, N.V.dos., Amorim, M.T.A., Demattê, J.A.M., 2021. Soil degradation index developed by multitemporal remote sensing images, climate variables, terrain and soil atributes. J. Environ. Manage. 277, 111316.

Neckel, A., Costa, C., Mario, D.N., Sabadin, C.E.S., Bodah, E.T., 2017. Environmental damage and public health threat caused by cemeteries: a proposal of ideal cemeteries for the growing urban sprawl. Urbe 9 (2), 216–230.

Neckel, A., Korcelski, C., Kujawa, H.A., Silva, I.S.da., Prezoto, F., Amorin, A.L.W., Maculan, L.S., Gonçalves, A.C., Bodah, E.T., Bodah, B.W., 2021. Hazardous elements in the soil of urban cemeteries; constructive solutions aimed at sustainability. Chemosphere 262, 128248.

Neckel, A., Silva, J.L.da., Saraiva, P.P., Kujawa, H.A., Araldi, J., Paladini, E.P., 2020. Estimation of the economic value of urban parks in Brazil, the case of the City of Passo Fundo. J. Clean. Prod. 264, 121369.

Nega, W., Hailu, B.T., Fetene, A., 2019. An assessment of the vegetation cover change impact on rainfall and land surface temperature using remote sensing in a subtropical climate, Ethiopia. Remote Sens. Appl. Soc. Environ. 16, 100266.

Oliveira, M.L.S., Neckel, A., Pinto, D., Maculan, L.S., Zanchett, M.R.D., Silva, L.F.O., 2021. Air pollutants and their degradation of a historic building in the largest metropolitan area in Latin America. Chemosphere 277, 130286.

PMPF (City Hall of Passo Fundo), 2021. Passo Fundo Against Coronavirus. http://www.pmpf.rs.gov.br/secretaria.php?c=1360.

Prangnell, J., Mcgowan, G., 2009. Soil temperature calculation for burial site analysis. Forensic Sci. Int. 191 (3), 104–109.

Rae, R.A., 2021. Cemeteries as public urban green space: management, funding and form. Urban For. Urban Green. 61, 127078.

Rodriguez-Galiano, V., Pardo-Iguzquiza, E., Sanchez-Castillo, M., Chica-Olmo, M., Chica-Rivas, M., 2012. Downscaling Landsat 7 ETM+ thermal imagery using land surface temperature and NDVI images. Int. J. Appl. Earth Obs. Geoinf. 18, 515–527.

Romer, I., White, T.A., Baalousha, M., Chipman, K., Viant, M.R., Lead, J.R., 2011. Aggregation and dispersion of silver nanoparticles in exposure media for aquatic toxicity tests. J. Chromatogr. A. 1218, 4226–4233.

Rosmorduc, V., Srinivasan, M., Richardson, A., Cipollini, P., 2020. The first 25 years of altimetry outreach. Adv. Space Res., 1–12

Sayão, V.M., Santos, N.V.dos., Mendes, W.de.S., Marques, K.P.P., Safanelli, J.L., Poppiel, R.R., Demattê, J.A.M., 2020. Land use/land cover changes and bare soil surface temperature monitoring in southeast Brazil. Geoderma Reg. 22, e00313.

Silva, L.F.O., Pinto, D., Neckel, A., Dotto, G.L., Oliveira, M.L.S., 2020. The impact of air pollution on the rate of degradation of the fortress of Florianópolis Island, Brazil. Chemosphere 251, 126838.

Silva, L.F.O., Santosh, M., Schindler, M., Gasparotto, J., Dotto, G., Oliveira, M.L.S., Hochella, M., 2021. Nanoparticles in fossil and mineral fuel sectors and their impact on environment and human health: a review and perspective. Gondwana Res. 92, 184–201.

Shao, L., Ge, S., Jones, T., Santosh, M., Silva, L.F.O., Cao, Y., Oliveira, M.L.S., Zhang, M., Bérubé, K., 2021. The role of airborne particles and environmental considerations in the transmission of SARS-CoV-2. Geosci. Front., 101189

Shi, Y., Liu, S., Yan, W., Zhao, S., Ning, Y., Peng, X., Chen, W., Chen, L., Hu, X., Fu, B., 2021. Influence of landscape features on urban land surface temperature: scale and neighborhood effects. Sci. Total Environ., 145381

Stern, R.A., Al-Hemoud, A., Alahmad, B., Koutrakis, P., 2021. Levels and particle size distribution of airborne SARS-CoV-2 at a healthcare facility in Kuwait. Sci. Total Environ., 146799

Sussman, H.S., Raghavendra, A., Zhou, L., 2019. Impacts of increased urbanization on surface temperature, vegetation, and aerosols over Bengaluru, India. Remote Sens. Appl. Soc. Environ. 16, 100261.

Toscan, P.C., Neckel, A., Korcelski, C., Maculan, L.S., Maroni, D., Fuga, T.M., Cambrussi, L.P., Kujawa, H.A., Bodah, E.T., Bodah, B.W., 2020. Urban Cemeteries in Southern Brazil: an analysis of planimetric variations, vegetation indices and temperature. J. Civ. Eng. Arc. 14 (11), 617–624.

USGS (United States Geological Survey), 2021. Mapping, Remote Sensing, and Geospatial Data. https://www.usgs.gov/science/science-explorer/Mapping%2C+Remote+Sensing%2C+and+Geospatial+Data.

Vanhellemont, Q., 2020. Combined land surface emissivity and temperature estimation from Landsat 8 OLI and TIRS. ISPRS J. Photogramm. Remote Sens. 166, 390–402.

Wanderley, R.L.N., Domingues, L.M., Joly, C.A., Rocha, H.R.da., 2019. Relationship between land surface temperature and fraction of anthropized area in the Atlantic forest region, Brazil. Plos One 14 (12), 1–19.

WHO (World Health Organisation), 2021. WHO Coronavirus Disease (COVID-19) Dashboard. https://covid19.who.int/.

Wu, Z., Yao, L., Zhuang, M., Ren, Y., 2020. Detecting factors controlling spatial patterns in urban land surface temperatures: a case study of Beijing. Sustain. Cities Soc. 63, 102454.

Yang, J., Ren, J., Sun, D., Xiao, X., Xia, J., Jin, C., Li, X., 2021. Understanding land surface temperature impact factors based on local climate zones. Sustain. Cities Soc. 69, 102818.

Zullo, F., Fazio, G., Romano, B., Marucci, A., Fiorini, L., 2019. Effects of urban growth spatial pattern (UGSP) on the land surface temperature (LST): A study in the Po Valley (Italy). Sci. Total Environ. 650, 1740–1751.

Zhu, N., Zhang, D., Wang, W., Li, X., Yang, B., Song, J., Zhao, X., Huang, B., Shi, W., Lu, R., 2020. A Novel Coronavirus from Patients with Pneumonia in China, 2019. N. Engl. J. Med. 382 (8), 727–733.

Zorzi, C.G.C., Neckel, A., Maculan, L.S., Cardoso, G.T., Moro, L.D., Savio, A.A.D., Carrasco, L.D.Z., Oliveira, M.L.S., Bodah, E.T., Bodah, B.W., 2021. Geo-environmental parametric 3D models of SARS-CoV-2 virus circulation in hospital ventilation systems. Geosci. Front., 101279